AIAA JOURNAL
Vol. 40, No. 1, January 2002

Study of Direct-Measuring Skin-Friction Gauge with Rubber Sheet for Damping

Samantha Magill,* Matthew MacLean,* Joseph Schetz,†
Rakesh Kapania,‡ Alexander Sang,* and Wade Pulliam§
Virginia Polytechnic Institute and State University, Blacksburg, Virginia 24061

This study concerns the direct measuring technique for skin-friction determination. Such a device measures the force on a small, movable surface element as a shear flow passes over the surface. The typical direct-measuring skin-friction gauge uses a viscous liquid in the gap between the movable surface piece and the casing to dampen vibrations, to create an even surface, to minimize the effects of pressure gradients, and for temperature stabilization. In testing, the liquid slowly leaks out. Therefore, we have considered gauges with rubber to fill all or some of the gap. This led to the development of a gauge with a thin rubber sheet to cover the face of the gauge instead of a previous design with rubber filling the entire internal volume. First, a finite element method model was employed to fully understand the strain field involved and to finalize the design. The resulting design consisted of a plastic skin friction gauge with a 12.7-mm-diam floating element on a cantilever beam flexure, an approximately 0.51-mm-thick rubber sheet, a 1.6-mm-wide gap around the floating element on a cantilever beam flexure, and semiconductor strain gauges at the beam base. Vibration tests were performed to determine if this design produced the required damping. These tests were successful. Supersonic wind-tunnel tests at Mach 2.4 with a total pressure of 3 atm and ambient total temperature demonstrated that the rubber sheet survived repeated tests and provided adequate damping. The skin-friction data obtained compared well with theory and other measurements.

Nomenclature

A	=	area
C	=	calibration ratio
C_f	=	skin-friction coefficient
d	=	diameter
E	=	Young's modulus
F	=	force
G	=	shear modulus
g	=	gravity
h	=	height
I	=	moment of inertia
k	=	spring constant
L	=	length
P_0	=	total pressure
p	=	static pressure
R	=	resistivity
U	=	edge velocity
u_*	=	friction velocity
V	=	voltage
ε	=	strain
ζ	=	modal damping coefficient
λ	=	shear correction factor
ρ	=	density
τ_w	=	wall shear

Received 7 July 2000; revision received 20 May 2001; accepted for publication 8 June 2001.

*Graduate Research Assistant, Aerospace and Ocean Engineering Department. Student Member AIAA.
†Fred D. Durham Chair, Aerospace and Ocean Engineering Department. Fellow AIAA.
‡Professor, Aerospace and Ocean Engineering Department. Associate Fellow AIAA.
§Graduate Research Assistant, Aerospace and Ocean Engineering Department; currently Research Engineer, University of California, Los Angeles, Los Angeles, CA 90024. Member AIAA.

Introduction

THE knowledge of skin-friction drag or any other drag is vital in the understanding of the performance of a fluid engineering system "whether it be a ship or an aircraft or the flow through a pipe."[1] Skin friction is most commonly expressed as a coefficient of wall shear stress,

$$C_f = \tau_w \Big/ \tfrac{1}{2}\rho U^2 \tag{1}$$

Skin friction is also a vital component in research on turbulent boundary layers. It is involved with u_* which is a scaling velocity used in the correlation of turbulent boundary-layer velocity profiles and is defined as

$$u_* = U\sqrt{C_f/2} \tag{2}$$

These correlations and u_* are critical to the development of all turbulent transport models, which are used in virtually every computational fluid dynamics (CFD) code.

Measurements of skin friction date at least as far back as Beaufoy in 1793.[2] Some of the first systematic investigations of drag were made by Froude in 1872, who measured the shear forces on a series of planks towed at various speeds along a tank.[1] Over the years various techniques have been tried. Indirect methods for measuring skin friction were more feasible in the early studies. As technology advanced, direct measurements of skin friction became more useful and commonplace. Wooden and Hull[3] categorize these techniques according to the physical quantity being measured. The direct method utilizes a measurement of the wall shear force without assumptions that might require some prerequisite knowledge about the flow. This method relies on a floating element that is not intrusive into the flow. Winter[1] detailed the history of early measurement of skin friction with direct methods. A discussion of more recent work can be found in Schetz.[4] Magill[5] combines early and recent work as well as providing additional historical information on direct measuring skin-friction techniques.

Indirect methods are based on the measurement of other flow quantities that are then related back to the skin friction. All but the newest of the methods are reviewed in Winter,[1] Wooden and Hull,[3] and Nitsche et al.[6] These methods use a variety of analytical correlations to relate the measured property to a skin-friction coefficient, which requires substantial prior knowledge of the flow. They are not yet considered reliable in complex flows, three-dimensional cases,

unsteady flows, flows with suction or injection, rough wall cases or high-speed flows with heat addition and/or shocks. Some commonly used instruments for indirect measurement are the pitot tube (Preston and Stanton), the hot-wire anemometer, the surface hot-film anemometer, and the interferometer with a surface oil films. The surface hot-film techniques measure heat transfer and then employ Reynolds analogy. They are sometimes grouped separately from indirect measurements. Liquid crystals are another type of indirect method; they are an optically active mixture that reflects light at a particular wavelength in response to a physical stimuli. Liquid crystals are generally considered more qualitative and are, therefore, well suited for locating transition. There has also been considerable recent interest in the use of an interferometer to measure the time history of the thickness of oil surface film to deduce wall shear. The errors and limitations of indirect methods are mostly caused by the difficulty of the instrumentation, but also to the assumptions, additional calculations, and/or inferences of the flowfield used to determine the skin friction.[1,3,6] Wooden and Hull[3] developed a chart listing the advantages and disadvantages of direct methods, indirect methods, and Reynolds analogy; the chart is shown in Table 1. Because our work deals with direct measurement techniques of skin friction, there will be no further discussion of indirect methods or Reynolds analogy.

The direct method is divided into nulling and nonnulling designs. In a nulling design the sensing element is returned to its original, or null, position by a restoring force that is equal to the shear force. A variety of nulling gauges have been developed, but they all have drawbacks. First, they have a slow time response. Second, because of the mechanical complexities of the device, problems with fabrication, assembly, size, and robustness are issues. The nulling technique is also generally restricted to two-dimensional, unheated flows.

In a nonnulling design the sensing element is allowed to deflect slightly under the shearing load, yet the deflections are limited so that the floating element does not protrude into the flow. The effects of head protrusion, gap size, etc., on skin-friction measurements have been documented by Allen.[7] See Fig. 1 for an example of a nonnulling design.

Generally, the sensing element consists of a floating head mounted on a cantilever beam flexure. The strain is measured at the base of the cantilever beam by strain gauges, and that strain is related to the shear force at the sensing head. Strain gauges are configured as a Wheatstone Bridge and relate a change in resistance, associated with a change in length of a specimen, to a change in strain through voltage output. A nonnulling configuration allows for a design that is uncomplicated in fabrication and maintenance. This design also yields a skin-friction gauge of a size manageable for engineering applications. This arrangement allows for the measurement of both components of the shear in the plane of the wall, by using two sets of strain gauges on the base of the beam. The nulling designs generally cannot accomplish that.

Earlier direct-measurement skin-friction gauges developed at Virginia Polytechnic Institute and State University employed a vis-

Table 1 Overview of skin-friction measurement techniques (adapted from Wooden and Hull[3])

Method	Advantages	Disadvantages
Direct measurement (force)	Most believable	Tare sensitive
	High-precision measurement	Small force
		High cost
	High-precision calibration	Large size (inside model)
	Direction sensitive	Direction sensitive
Indirect measurements (laminar sublayer total pressure)	Simple	Flow calibration required
	Low cost (after calibration)	Medium precision curve fit
		Minimum boundary-layer thickness limited
	High-precision measurement	Direction sensitive
Reynolds analogy (thermal measurement)	Dual-purpose sensor	Calibration not available
	Low cost	Low precision measurement
	Not direction sensitive	Boundary-layer edge conditions required
		Not direction sensitive

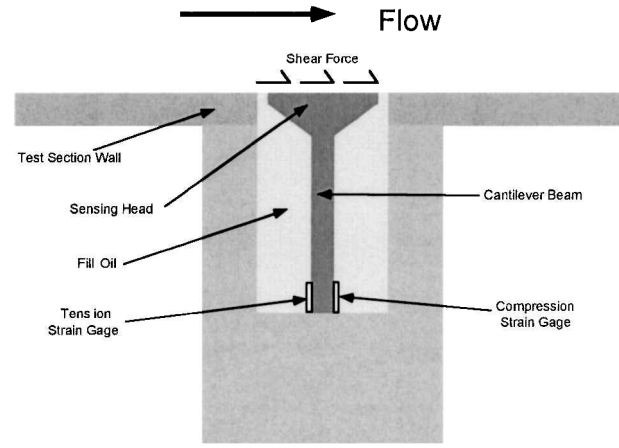

Fig. 1 Direct method nonnulling gauge concept.

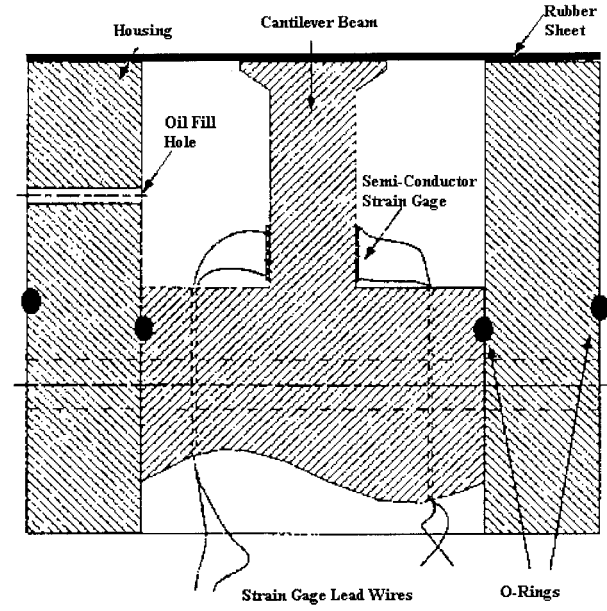

Fig. 2 Nonnulling skin-friction gauge with rubber sheet to provide damping and retain the fill liquid.

cous liquid in the internal volume for four purposes. First, the liquid in the small gap around the floating element provides a continuous surface to the external flow making the floating element nonintrusive. Second, the incompressible liquid minimizes the effects of pressure gradients. Third, it helps in thermal stabilization and protection of the skin-friction gauge and strain gauges. Fourth, the liquid reduces the effects of vibrations by providing strong viscous damping. A significant disadvantage to the liquid fill is that it slowly leaks out over time even with the small gaps (0.10 mm nominal) around the floating head. This means that the gauge requires frequent inspection and servicing.

Some work was done with a rubber fill replacing the oil.[8] This gauge concept did have the advantage of eliminating the oil leakage problem as well as good vibration characteristics, but it had disadvantages. The sensitivity was reduced, and a much larger gap was required around the floating head. This design was also not as successful as a liquid fill in reducing the effects of pressure gradients. Finally, calibration is more complex because the shear force acting on the rubber in the gap is transmitted to the beam.

The new concept that was investigated here is an arrangement where a thin rubber sheet covers the floating head of the gauge, the gap around the head, and the surrounding housing. The interior of the gauge under the rubber sheet may or may not have a viscous liquid fill. See the sketch in Fig. 2.

Semiconductor strain gauges were employed because they have a gauge factor of 135–150, a hundred times greater than conventional metal foil strain gauges, that allows them to measure very small

deflections. Semiconductor strain gauges operate on the theory of piezoresistivity, which relates the change of electrical resistance to applied stress or pressure. Because of the large gauge factor, the temperature sensitivity of semiconductor strain gauges is also amplified over conventional strain gauges; therefore, an in-line temperature compensation unit was added to minimize changes in resistance as a result of temperature.

For this work an excitation of 1.0 V and a gain of 1.0 were set for the semiconductor strain gauges to minimize noise even though these settings produced a small output voltage, 0.1 to 1.0 mV. Such a small voltage output requires a minimum of 16-bit data acquisition board. On an additional note, a signal conditioning unit, which has multiple functions, was connected to the strain gauges for the purpose of supplying the excitation voltage, balancing effects (a tare), filtering, and gain.

Design of Rubber Sheet Skin-Friction Gauge

The goals of this skin-friction gauge development were to eliminate oil leakage, dampen vibrations, and be easily calibrated. But, instead of filling the entire gap with silicone rubber, simply cover it with a thin silicone rubber sheet, and fill the gap with the usual silicone oil. The idea sounds promising, but several questions had to be answered before the design could be realized. First, is it possible to fabricate a suitable thin silicone rubber sheet? Second, how thin is "thin enough" for the silicone rubber sheet? One wants a sheet that will retain the oil and remain intact during testing, but not so thick that it inhibits the shear load distribution or bears a substantial part of the shear load compared to that in the cantilever beam. And third, how wide is the necessary gap between the floating head and the gauge housing? Clearly, the size of the gap plays together with the sheet thickness in determining the load borne by the sheet.

Before the last two questions could be answered, a baseline design of the skin-friction gauge had to be chosen. A plastic gauge similar in arrangement to an earlier gauge used by Novean et al.[8] but now designed for a nominal shear level of 100 Pa was developed using simple beam theory and our existing knowledge base. The entire skin-friction gauge was built of polyethersulfone (PES) high-temperature plastic to reduce thermal expansion, which also deterred unwanted thermal resistance changes in the strain gauge. The cantilever beam flexure for this design is depicted in Fig. 3. The parameters for the housing of the gauge were determined with the optimization of the rubber thickness and gap size.

The finite element program ABAQUS was used to produce a finite element model of a skin-friction gauge with a sheet of silicone rubber in order to address the last two questions just posed. The goals of this model were to simulate how the rubber sheet, the cantilever beam, and the housing deform with imposed shear stresses. ABAQUS has an extensive library of elements to suit virtually any geometry, as well as a list of material models to simulate anything from metal to resilient foam. The input had approximately 5500 elements consisting of brick elements with eight nodes and pie elements with six nodes to model the skin-friction gauge; a concentrated load was applied at each node exposed to the shear stress. All elements were chosen to be compressible, except for the silicone rubber sheet. The proper choice for the silicone rubber sheet is what ABAQUS calls a hybrid element type, designated with an H (e.g., C3D8H, which is a continuum, three-dimensional, eight-node, hybrid element). A hybrid element is chosen when the material is incompressible (Poisson's ratio = 0.5) or almost incompressible (0.48 ≥ Poisson's ratio < 0.5). The two-part silicone rubber used here has a Poisson's ratio of 0.495; therefore, a hybrid element was necessary. Table 2 contains a brief list of applicable material properties for the three materials employed in this work, PES for the skin-friction gauge, silicone rubber, and glycerine (to be discussed later) for the filler liquid and the calibration rig. ABAQUS required material properties of the PES plastic and rubber. Additional details of the properties can be found in Magill.[5]

Before details of the analysis results are discussed, it is important to note the grid-refinement study that was performed. A grid-refinement study on any numerical method such as finite element analysis or CFD is very important to ensure accuracy. The grid refinement of the skin-friction gauge focused on the flexure and floating head assembly and the rubber sheet. In simple terms, rows of elements were added to first the beam, and then the rubber sheet until the strain at the beam base was constant to approximately a tolerance of 2.0%. Only a few trials were necessary, but it was apparent that the grid refinement was necessary because the addition of elements did initially change the value of strain at the beam base. The strain at the beam base is the most important because that is where the semiconductor strain gauges are located. Also, a small hole through the center of the beam was added. It was advised that multiple nodes at one location could be prone to error. More information on the techniques employed, grid size, and shape can be found in Magill.[5]

The first finite element run was with an empty gap (no rubber sheet) as a baseline, yielding a maximum strain at the beam base of 21.6 $\mu\varepsilon$. The next runs had various gap sizes with a fixed thickness for the rubber sheet. Figure 4 plots the variation of strain at the

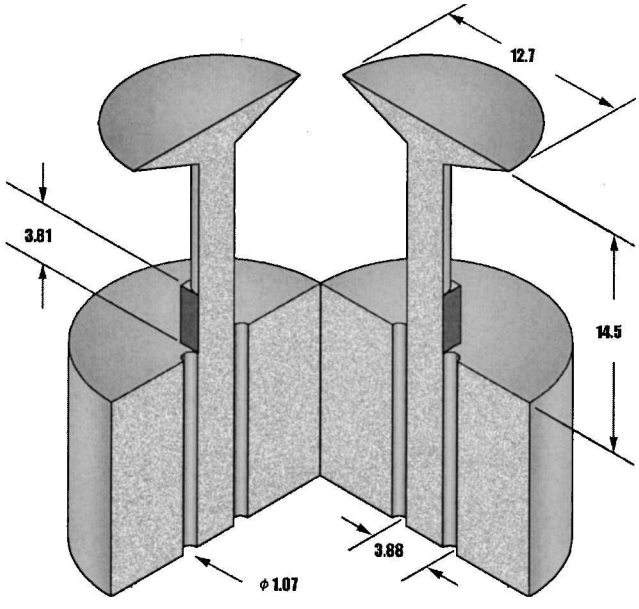

Fig. 3 Schematic of flexure piece for rubber sheet skin-friction gauge (all dimensions in millimeters).

Table 2 Relevant properties of materials in rubber sheet skin-friction gauge[5]

	Material		
Property	PES	Silicone rubber RTV566	Glycerine USP 99.7%
Viscosity, cp	——	——	1410
Density, kg/m^3	1384	1490	1260
Modulus of elasticity	2.66 GPa	552 kPa	——

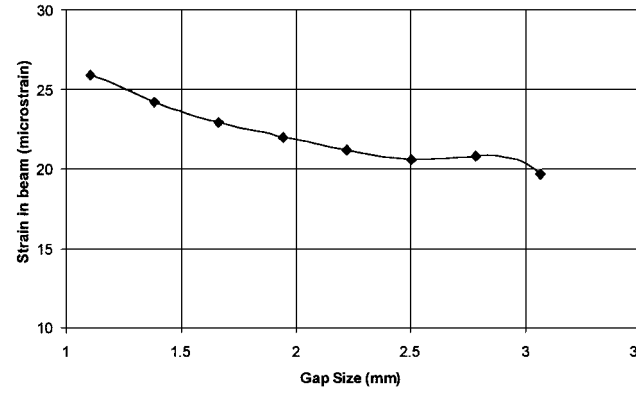

Fig. 4 Effect of gap size for a rubber sheet skin-friction gauge with a sheet thickness of 0.178 mm (0.007 in.). Axial strain is along the beam at the base.

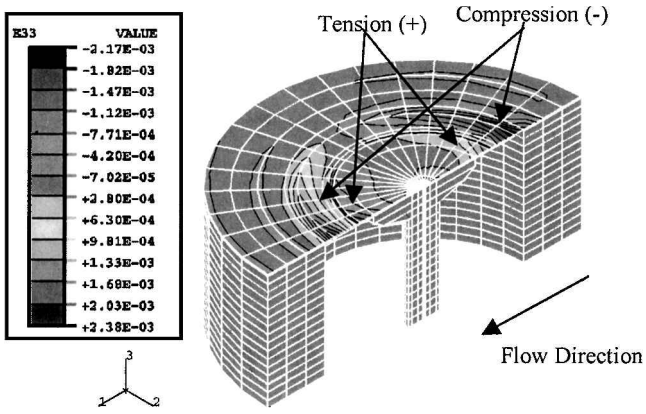

Fig. 5 Strain contour plot of rubber sheet skin-friction gauge with a gap size of 1.6 mm and a sheet thickness of 0.178 mm. Strain in the 3-direction.

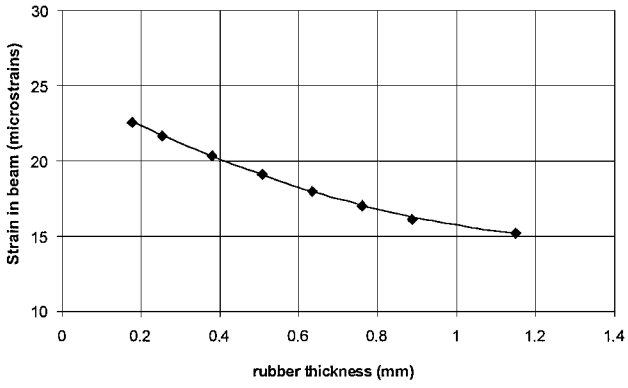

Fig. 6 Effect of rubber sheet thickness for a skin-friction gauge with gap size of 1.6 mm (0.0625 in.). Axial strain is along the beam at the base.

beam base in the vertical direction versus gap size for a 0.178-mm (0.007-in.)-thick silicone rubber sheet. The rubber sheet thickness of 0.178 mm was chosen because it was originally believed that the sheet could be manufactured to that thickness. The strain does not change dramatically with increasing gap size. The important part was that the gap size be reasonable to construct and adjoin to the rubber sheet. From these data a gap size of 1.6 mm (0.0625 in.) was considered suitable for construction. The maximum strain in the beam is only decreased slightly under these conditions. Figure 5 is a strain contour plot of the strain in the vertical (indicated as 3-direction in Fig. 5) for the gap size of 1.6 mm. Notice the variation in the strain across the rubber sheet acting in compression (negative) then tension (positive) on the right-hand side, but opposite on the left-hand side. The applied shear stress is indicated on Fig. 5 acting from right to left. The hole through the beam center just mentioned is also visible in Fig. 5.

Next, several rubber thicknesses were chosen from 0.178 to 1.14 mm (0.007 to 0.045 in.) with a gap size of 1.6 mm, and these values were implemented in ABAQUS. Figure 6 shows the results, where the variation in beam strain is acceptable for a rubber sheet thickness of up to about 0.5 mm (0.02 in.), which is the largest manufacturing thickness considered. The strain in the beam decreases more rapidly for an increase in the rubber sheet thickness than for an increase in gap size. Again, the strain documented is in the vertical or 3-direction.

The second and third questions of thickness and gap size posed at the beginning of this section have now been answered. The final gauge design had a 1.6-mm (0.0625-in.) gap and a nominal rubber sheet thickness of 0.38 mm (0.015 in.) The first question concerning forming a thin sheet was answered by fabrication trials. We found that silicone rubber sheets of 0.178–0.5-mm thickness could be reliably cured and adhered to the plastic floating head and housing by relatively simple techniques.

A simple analysis was also developed that can aid in the design. The beam supporting the floating head is taken as a cantilever beam, and the rubber sheet is modeled as a spring with a spring constant k attached perpendicular to the end of the cantilever beam. The strain at the base of the beam in response to a concentrated load F at the center of the floating head can then be written

$$\varepsilon_a = \frac{Fd(L-a)}{2EI_a}\left[\frac{1}{1+kL^3/3EI+k\lambda L/2AG}\right] \tag{3}$$

Equation (3) was derived from basic structural energy methods, and this expression can be used to determine the effective spring constant of a given rubber sheet by measuring the strain in the attached beam at a distance a from the beam base. That value of the spring constant can then be used in Eq. (3) to design a beam for a new gauge application using a similar rubber sheet.

Skin-Friction Gauge Calibration

The semiconductor strain gauges located on opposite sides of the cantilever beam yield a voltage output in response to a deflection in the beam. The response is linear for strain gauges; therefore, a simple static calibration can be performed. A known weight is attached parallel to the direction of flow and perpendicular to the floating head surface (Fig. 7). This simple method has worked extremely well with the skin-friction gauges filled with liquid. The effect of the shear stress acting on the liquid is negligible; therefore, a weight located at the head center and in the plane of the strain gauges is an accurate model of the flow for calibration. The effect of a shear stress acting on a rubber sheet is, however, not negligible. The shear force acts on the surface area of the silicone rubber as well as on the floating head of the gauge, and this increases the strain seen by the strain gauges. Thus, the aforementioned hanging weight calibration method is inappropriate. For an accurate calibration the known weight would have to be distributed evenly over the surface of the floating head and silicone rubber.

The calibration curves with the simple hanging weight method for the two skin-friction gauges used here are presented in Figs. 8 and 9. The calibration weight is converted to an equivalent shear by dividing by the area of the floating head. This is documented on the secondary axis in Figs. 8 and 9. The skin-friction gauge has to be calibrated in two directions. The weight acts with gravity having one side of the beam in tension and the other side of the beam in compression; that is one direction. Having the skin-friction gauge flipped with the opposite sides of the beam in compression and in tension is the other direction. These two directions are demonstrated in Figs. 8 and 9, as positive and negative slopes. Figure 8 is an accurate calibration because the gauges had no rubber sheet attached, but Fig. 9 shows a decrease in slope because one gauge then had a rubber

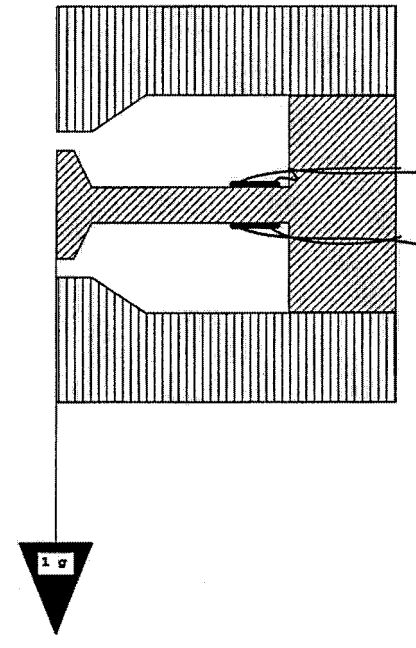

Fig. 7 Typical calibration of nonnulling skin-friction gauge.[5]

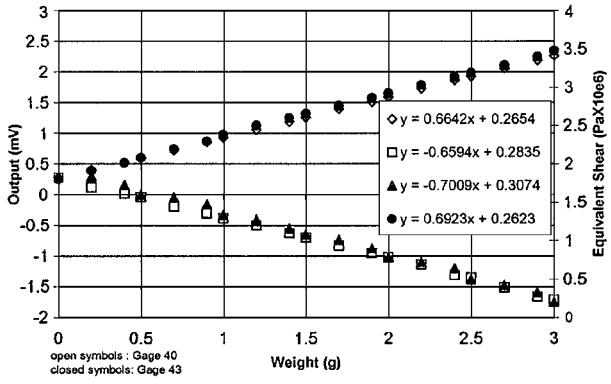

Fig. 8 Calibration of two skin-friction gauges without the rubber sheet using the hanging-weights method.

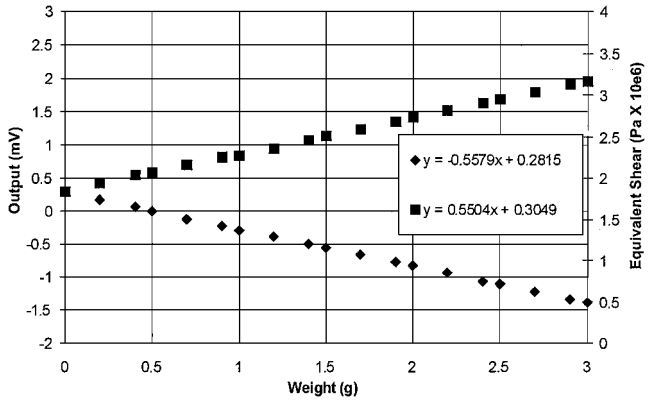

Fig. 9 Calibration of skin-friction gauge with rubber sheet using the hanging-weights method.

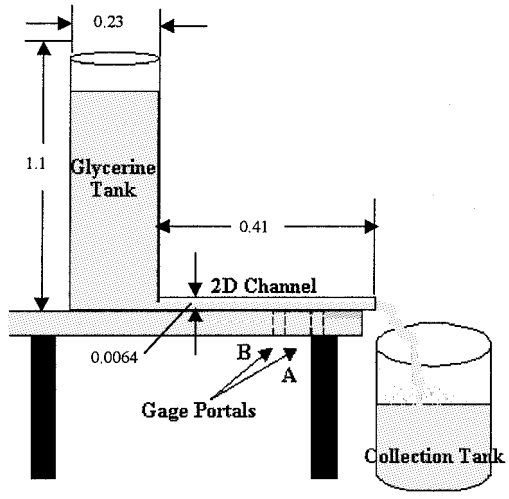

Fig. 10 Simple schematic of calibration rig (all dimensions in meters).

sheet attached. This decrease in sensitivity is expected because the rubber sheet takes some of the load. The calibration curves presented do not have a zero y-intercept because the excitation voltage is very low (1.0 V), again in order to limit noise and electrical heating.

To perform a proper calibration of the gauges with a rubber sheet attached, it is necessary to apply a known shear stress over the entire surface of the gauge. For this purpose we constructed a special calibration rig, where glycerine flows under fully developed conditions through a two-dimensional channel. See the simplistic schematic in Fig. 10. Fully developed flow is achieved at points far from the entrance of a channel flow, where the velocity profile is independent of axial motion. The channel is lined with pressure ports 2.54 cm (1.0 in.) apart, and one or two rubber filled skin-friction gauges lie flush with the floor toward the end of the channel. The collection tank keeps the glycerine from spilling, and the portals have fitted plugs and adapter pieces for when the portals are not in use and for different size skin-friction gauges. A large reservoir apparatus to supply the tank was built consisting of a 208-l (55-gallon) drum mounted to a wall approximately 1 m above the tank. It is connected to the tank with piping including an atmospheric outlet. The pressure distribution can then be measured, and the shear stress can be calculated using Eq. (4):

$$\tau_w = -\frac{\mathrm{d}p}{\mathrm{d}x}h \tag{4}$$

where h is the channel height measured from the centerline and $\mathrm{d}p/\mathrm{d}x$ is the pressure gradient. Equation (4) is derived by summing the forces acting on a fluid element and applying conservation of momentum.[9] For this particular case the pressure gradient is $\mathrm{d}p/\mathrm{d}x = 33.4$ Pa/mm (0.123 psi/in.), corresponding to a wall shear stress $\tau_w = 106$ Pa (0.0154 psi).

For the calibration rig a pressure sensor was chosen that could be mounted flush to the fluid flow itself, thus giving the highest frequency response possible. Each pressure sensor was calibrated with a dead-weight tester. The rig produced all of the data in a short period of time, approximately 5 s, and the data needed to be recorded accurately. For this task a computerized data acquisition system (DAQ) was developed. A PC was fitted with LabVIEW software and a 16-bit DAQ card. A LabVIEW program was written that read output voltage of the pressure sensors converting it to a pressure and read the voltage output of the semiconductor strain gauges of the skin-friction gauge converting it to a shear stress. For more information on this DAQ system, the pressure sensors, the calibration unit of the sensor, or details of the calibration rig design, see Ref. 5.

As already mentioned, the calibration rig was utilized to yield a calibration ratio, which was necessary because of the estimated 12–15% decrease in static sensitivity between the calibration of the silicone rubber sheet skin-friction gauge and the calibration without the rubber sheet. The calibration ratio is the ratio of the true calibration constant of the skin-friction gauge with a rubber sheet to the calibration constant of a skin-friction gauge without any gap filler. Novean et al.[8] determined a ratio of 3.17, which was very close to the geometric ratio of 3.22, for a gauge with the interior completely filled with silicone rubber. The geometric ratio is the ratio of the area of the gap covered with silicone rubber plus the floating head to the area of the floating head alone. This calibration ratio enables one to relate a calibration curve obtained with the hanging-weights method over a range of applied force to the real case of a shear applied over the head and rubber sheet.

A thin silicone rubber sheet was affixed to the skin-friction gauge, and it was placed in the rig for repeated runs. The shear stress in the calibration rig is known from Eq. (4). By knowing the true shear stress and the output from the semiconductor strain gauges, an effective area can be deduced:

$$\tau_w = VCg/A_{\mathrm{eff}} \tag{5}$$

where A_{eff} is the effective area and C (the slope from plots like Fig. 8) is the calibration constant for the skin-friction gauge. Calculations yielded a calibration ratio ($A_{\mathrm{eff}}/A_{\mathrm{head}}$) of 1.4, which can be compared to the geometric ratio of 1.56 for this gauge.

Also, using the output of the skin-friction gauge a comparison between the results of the calibration rig and that of the predicted strain at the beam base in the vertical direction from ABAQUS can be made. For the given geometry of the gauge, ABAQUS predicts a maximum strain between approximately 20 and 23 microstrains (see Figs. 4 and 6). The results from the calibration rig yielded 18.2 microstrains by utilizing Eq. (6):

$$E_{\mathrm{output}} = E_{\mathrm{excitaion}}GF\varepsilon/2 \tag{6}$$

This result demonstrates the usefulness of FEM for designing the present and future skin-friction gauges.

An uncertainty analysis on this skin-friction gauge design was performed, and the results are in Table 3, yielding an overall error of $\pm 2.8\%$ when a rms method employed. A brief explanation of some

Table 3 Uncertainty of rubber sheet skin-friction gauge

Type of uncertainty	Level of uncertainty, %
Calibration	
Forward rotation	±2.0
Axial rotation	±1.5
Calibration rig	±0.91
Hardware, geometry effects with ports[5]	
Calibration rig	±0.53
Measured variable errors[5]	
Data acquisition	
Zero drift	±0.5
Electric noise from computers, sensors, wires, and connectors	
Data reduction	
Truncation , curve fits	±0.5
Overall uncertainty (rms)	2.80

components of Table 3 is necessary. The forward and axial rotation refer to the alignment of the hanging weight during calibration (see Fig. 7). The forward rotation error is the error in rotation from vertical to horizontal in utilizing gravity for calibration, and the axial rotation error is the error in alignment with the strain-gauge plane. One wants the hanging weight to be exactly 90 deg from the horizontal and in the plane of the strain gauges.

The dynamic range of the skin-friction gauge is comparable with other skin-friction units for high speed flows. Knowing the gauge factor (~150), the excitation voltage (1 V), the resistance (750 Ω), and the standard equation for strain gauges [Eq. (7)], the maximum shear that could theoretically be measured is 1500 Pa:

$$\varepsilon = \Delta R/R_0 GF \tag{7}$$

but the flexure would be permanently deformed at those levels. The applications in which this skin-friction gauge is to be used is up to approximately 150 Pa, and the gauge was calibrated within that relative range. The maximum capacity of the strain gauges is not necessary. The minimum shear stress that can be measured is contingent on the zero deflection output voltage, approximately 0.3 mV [see Figs. 8 and 9, Eq. (6), and Hooke's law], and the smallest calibration weights available, determined to be between 3–4 Pa. This is well below any shear levels to be measured by this skin-friction gauge.

The response time of the skin-friction gauge is instantaneous to the human observer and certainly suitable for run times in the calibration rig and a supersonic tunnel of a few seconds. Skin-friction gauges of a similar arrangement can be derived with high-frequency response (10–20 kHz) for impulse facilities.[8]

Vibration Testing of Rubber-Sheet Skin-Friction Gauge

In utilizing any skin-friction gauge, the vibrations of the test facilities can produce background noise large enough to mask the desired signal and even cause damage to the skin-friction gauge; therefore, a type of damping must play an important role in the design. In the past most skin-friction gauges have accomplished enough damping by the gap being filled with a viscous liquid. The question arose, will the thin silicone rubber sheet without any silicone oil produce enough damping?

The equipment in the Modal Analysis Laboratory at Virginia Polytechnic Institute and State University was used to perform tests of the dynamic behavior of the gauge with and without the rubber sheet and a liquid fill. A typical dynamic response test utilizes an exciter, a transducer, a signal conditioning amplifier, and an analysis system. For these tests the exciter is a 333.62-N (75-lb) electromagnetic shaker, the transducer is an impedance head, and the analysis system is a dynamic signal analyzer. The skin-friction gauge is mounted directly to the impedance head, preferably at the center of mass. For more information on these testing facilities, see Ref. 5.

All vibration tests were done at 1- and 2-g with a random noise input over a frequency range from 0–3000 Hz. This frequency range was chosen because it corresponds to vibrations associated with testing facilities. The tests were done with two identical skin-friction

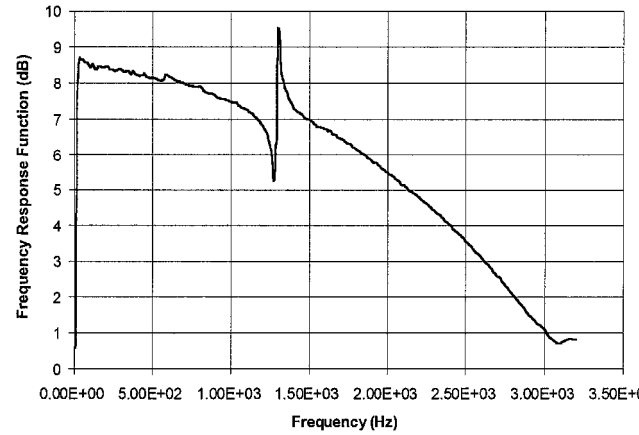

Fig. 11 Frequency response for skin-friction gauge without rubber sheet.

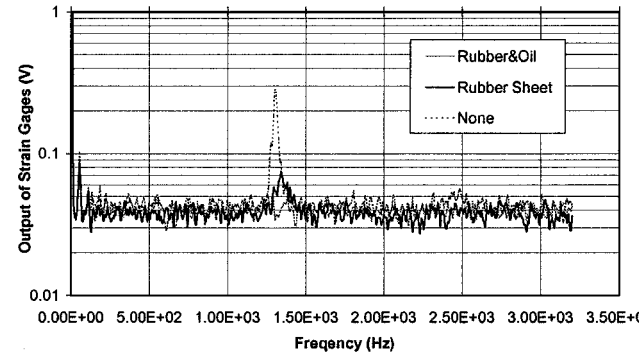

Fig. 12 Damping results for skin-friction without rubber sheet, with rubber sheet, and with rubber sheet plus oil.

gauges. The calibration curves of these two skin-friction gauges are in Fig. 8. One skin-friction gauge was used as a control, and the gap remained empty (designated as gauge 43). A second skin-friction gauge was tested with an empty gap (designated gauge 40), then the thin silicone rubber sheet was affixed across the top, and finally the gauge was also filled with silicone oil. Figure 11 displays the frequency response of the skin-friction gauge, which measures the output of the force transducer not the strain gauges. The natural frequency occurs at an infinite slope $\omega_n \approx 1.3$ kHz, which is in good agreement with a simple analytical estimate by modeling the skin-friction gauge flexure as a cantilever beam. The very small peak at approximately 600 Hz in Fig. 11 is attributed to error in the skin-friction gauge not being mounted to the shaker exactly at the center of mass. The data in Fig. 11 are considered adequate because of the limitations in manually adhering a connector to the center of mass; the connector must be completely removed for further testing of the skin-friction gauge in different facilities.

Figure 12 also shows the natural frequency and vibration response of skin-friction gauge by plotting the output of the strain gauges over the frequency range: without any gap filler or rubber sheet, with the thin silicone rubber sheet applied, and finally with the rubber sheet and gap filled with silicone oil, all shaken at 2-g. The dynamic tests of the skin-friction gauge with the rubber sheet produced excellent results. The primary peak was greatly damped, while the natural frequency shifted to the right slightly, which is to be expected, at $\omega_n = 1.344$ kHz. The silicone oil provided some additional damping.

These results can be interpreted in two ways. First, one can look at the reduction in peak output at the natural frequency. We determined a peak output of 0.28 mV for the gauge without a rubber sheet or liquid fill, a reduction to 0.07 mV for the gauge with the rubber sheet but no liquid fill, and a further reduction to 0.05 mV for the gauge with a rubber sheet and viscous liquid fill. The last value is at the level of the background noise. Second, one can consider the results in terms of the modal damping coefficient ζ using the method of

logarithmic decrement. We found $\zeta = 0.014$ for the gauge without a rubber sheet or liquid fill and an increase to $\zeta = 0.052$ for the gauge with the rubber sheet but no liquid fill. There is no clearly discernible peak for the gauge with a rubber sheet and viscous liquid fill so a numerical value for ζ could not be found, but the damping is obviously greater. The resonant frequency is approximately equal to the natural frequency because of the small, but effective, damping coefficient. These damping results compare favorably with viscous liquid fill, passive piezoelectric and magnetic damping concepts, and the present design is certainly much simpler.

Tests in the Supersonic Wind Tunnel

A number of tests have been run in the Virginia Polytechnic Institute and State University (VPISU) supersonic wind tunnel to analyze the performance of this new skin-friction gauge design. The tests were run at Mach 2.4 with a nominal total pressure of 3 atm (45 psia) and a total temperature of 300 K. Additional information on the VPISU supersonic tunnel is accessed on the departmental website at http://www.aoe.vt.edu/aoe/pysical/superson.html (15 May 2001). Basic information from the tunnel such as run time, stagnation and static pressure, temperature, etc. is constantly read through a PC fitted with LabView software. For this work the LabView program was modified to incorporate the voltage output readings of the strain gauges as shear stresses.

A half-nozzle configuration with a flat wall replacing the usual nozzle centerplane was employed so as to produce a constant pressure "flat plate." Measurements of the boundary-layer thickness were used in conjunction with the Blasius skin-friction law[9] and a Van Driest compressibility correction[9] to produce a prediction of the skin friction to be expected. Measurements with earlier, oil-filled skin-friction gauges are also available for comparison. The predictions and earlier data indicate $C_f = 0.0019$ at these conditions.

The first test series showed that the violent process of tunnel start and unstart could tear the rubber sheet off the gauge. Tunnel unstart was the worst condition. Following that experience, more attention was paid to carefully adhering the rubber sheet to the gauge surface. Other operational problems were identified and overcome. First, in order to maintain the rubber sheet as a flat surface over the gap during the reduced pressure conditions of the supersonic tunnel run we fill the space under the sheet and inside the gauge housing with liquid. Second, glycerine has now replaced our normal silicone oil as the fill liquid because silicone oil attacks the silicone rubber sheet. However, in our early attempts we found it difficult to remove all of the air in small bubbles and/or dissolved in the glycerine. We did fill the gauge under vacuum to try and remove all of the air, but we were not fully successful at that stage. If one then exposed only the active face of the gauge to a vacuum, deformation of the sheet caused by trapped air could be observed. The strain gauges also indicated loading of the cantilever beam. Obviously, steps had to be taken to remove all of the air from the inside of the gauge. That problem was solved by making small pin pricks in the rubber sheet with a sharp needle. These holes are small enough to prevent leakage of the glycerine, but large enough to allow any trapped air to escape when the gauge is exposed to a vacuum. Last, the sheet thickness was increased to a nominal 0.5 mm (0.020 in.) for greater robustness. Then, to maintain sensitivity of the gauge the gap around the head was increased such that the geometric area ratio (area of the head plus gap divided by that of the head) became 3.17. Tests in the calibration rig yielded an effective area ratio of 2.05. Using Eq. (3), we deduced an effective spring constant for this rubber sheet of 101 N/mm (577 lb/in.). With all of these improvements, the gauges proved capable of numerous runs in the supersonic tunnel.

A typical test result is given in Fig. 13. One can see the total pressure variation achieved by the control valve and the corresponding skin-friction output. The unfiltered skin-friction gauge output and an 11-point running average are shown. The average value tracks with the total pressure variation, as it should, and the average value during the period of relatively constant total pressure agrees very closely with the predicted value of $C_f = 0.0019$. The violent load produced by the passage of the tunnel starting shock is effectively damped. Finally, the noise floor of the gauge represented by the output signal before flow initiation can be seen to be small compared to the output signal.

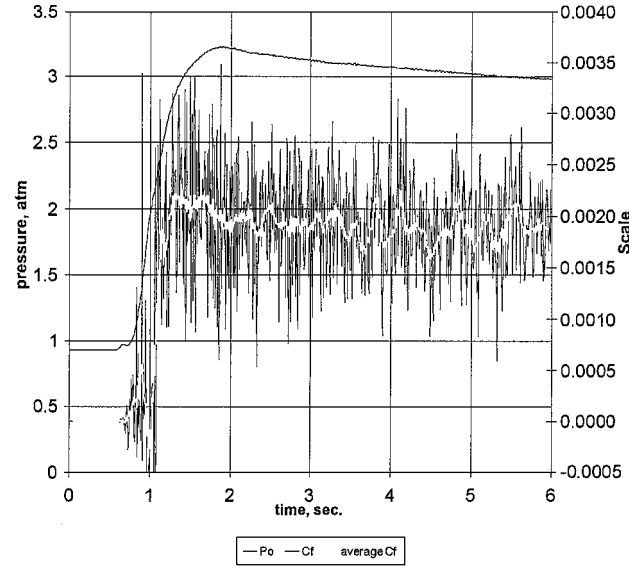

Fig. 13 Sample output from VPISU supersonic wind-tunnel tests at $M = 2.4$ with $P_0 = 3$ atm and $T_0 = 300$ K.

Conclusions

The objective of this work was to develop a new direct-measuring skin-friction gauge design that eliminated the operational problems associated with conventional designs that employ a viscous liquid fill. The liquid fill tends to leak out slowly over time, even with the small gaps (0.0254–0.102 mm) commonly used around the floating head. In situations where access to the test article is restricted in the laboratory or in flight tests, the need to inspect and refill the gauge is a serious limitation. At the same time any new gauge concept must provide adequate damping.

The new concept studied here involves placing a thin rubber sheet over the floating head, the gap around the head, and the top of the gauge housing. The interior below the rubber sheet may or may not be filled with liquid. First, the design of such a gauge was investigated using detailed finite element analysis. The results were very promising. Second, laboratory vibration tests proved that adequate damping was achieved even without a liquid fill. Indeed, the rubber sheet provided damping that compared very favorably with more complex alternatives such as passive piezoelectric or magnetic damping. Third, the matter of calibration and how the shear from the flow acting on the rubber sheet affected calibration were considered. A satisfactory calibration procedure was developed. Fourth, fabrication issues had to be addressed, and successful methods were found and employed. It was learned that minute holes placed in the rubber sheet were very helpful in eliminating problems caused by trapped gases when the interior of the gauge was filled with viscous liquid. Last, the gauges were tested under supersonic, high-Reynolds-number conditions in a wind tunnel. The gauges proved robust even under the violent tunnel start and unstart processes. In addition, the numerical values for skin-friction coefficient obtained agreed well with predictions and other measurements.

The tools developed and demonstrated here can be used to design skin-friction gauges of this type for a wide variety of applications. This skin-friction gauge concept measures both components of the wall shear in the plane of the wall. It can also be easily adopted for curved surfaces. Finally, it can be expected to minimize the effects of pressure gradients because no flow can be induced in the gap around the floating head or the interior of the gauge.

Acknowledgment

This work was supported by Luna Innovations, Inc., as part of a project funded by the U.S. Air Force Research Laboratory in Dayton, Ohio.

References

[1]Winter, K. G., "An Outline of the Techniques Available for the Measurement of Skin Friction in Turbulent Boundary Layers," *Progress in Aerospace Sciences*, Vol. 18, 1977, pp. 1–57.

[2]Chapman, D. R., and Kester, R. H., "Measurements of Turbulent Skin Friction on Cylinders in Axial Flow and Subsonic and Supersonic Velocities," *Journal of the Aeronautical Sciences*, Vol. 20, No. 7, 1953, pp. 441–448.

[3]Wooden, P. A., and Hull, G. H., "Correlation of Measured and Theoretical Heat Transfer and Skin Friction at Hypersonic Speeds Including Reynolds Analogy," AIAA Paper 90-5244, 1990.

[4]Schetz, J. A., "Direct Measurements of Skin Friction in Complex Flows," *Applied Mechanics Review*, Vol. 50, No. 11, Pt. 2, Nov. 1997, pp. 198–203.

[5]Magill, S. A., "Study of a Direct Measuring Skin Friction Gage with Rubber Compounds for Damping," M.S. Thesis, Aerospace and Ocean Engineering Dept., Virginia Polytechnic Inst. and State Univ., Blacksburg, VA, July 1999.

[6]Nitsche, W., Haberland, C., and Thunker, R., "Comparative Investigation on Friction Drag Measuring Techniques in Experimental Aerodynamics," International Council of the Aeronautical Sciences, Paper 84-2.4.1, Sept. 1984.

[7]Allen, J. M., "Improved Sensing Element for Skin-Friction Balance Measurements," *AIAA Journal*, Vol. 18, No. 11, 1980, pp. 1342–1345.

[8]Novean, M. G., Schetz, J. A., and Bowersox, R. D. W., "Direct Measurement of Skin Friction in Complex Supersonic Flows," AIAA Paper 97-0394, Jan. 1997.

[9]Schetz, J. A., *Boundary Layer Analysis*, Prentice–Hall, Upper Saddle River, NJ, 1993, Chaps. 2, 5, 8.

J. P. Gore
Associate Editor